Cell PRESS
Immunity
Article

Persistent Antigen and Germinal Center B Cells Sustain T Follicular Helper Cell Responses and Phenotype

Dirk Baumjohann,[1,2,3,*] Silvia Preite,[1] Andrea Reboldi,[1,4] Francesca Ronchi,[1] K. Mark Ansel,[2,3] Antonio Lanzavecchia,[1] and Federica Sallusto[1,*]
[1]Institute for Research in Biomedicine, Via Vincenzo Vela 6, 6500 Bellinzona, Switzerland
[2]Department of Microbiology & Immunology
[3]Sandler Asthma Basic Research Center
University of California, San Francisco, San Francisco, CA 94143, USA
[4]Present address: Howard Hughes Medical Institute and Department of Microbiology & Immunology, University of California, San Francisco, San Francisco, CA 94143, USA
*Correspondence: dirk.baumjohann@ucsf.edu (D.B.), federica.sallusto@irb.usi.ch (F.S.)
http://dx.doi.org/10.1016/j.immuni.2012.11.020

SUMMARY

T follicular helper (Tfh) cells provide help to B cells and are crucial for establishment of germinal center (GC) reactions, including production of high-affinity antibodies and generation of memory B cells and long-lived plasma cells. Here we report that the magnitude of the Tfh cell response was dictated by the amount of antigen and directly correlated with the magnitude of the GC B cell response. In addition, maintenance of the Tfh cell phenotype required sustained antigenic stimulation by GC B cells. In lymphopenic conditions, a strong and prolonged Tfh cell response led to bystander B cell activation, hypergammaglobulinemia, and production of poly- and self-reactive antibodies. These data demonstrate that antigen dose determines the size and duration of the Tfh cell response and GC reaction, highlight the transient nature of the Tfh cell phenotype, and suggest a link between overstimulation of Tfh cells and the development of dysregulated humoral immune responses.

INTRODUCTION

T-cell-dependent antibody responses require the coordinated interplay of many different cell types, including dendritic cells (DCs), B cells, and T cells, in highly specialized secondary lymphoid organ structures (Crotty, 2011; Goodnow et al., 2010; McHeyzer-Williams et al., 2011). Whereas T cell activation in the T cell zone is mediated by antigen-presenting DCs (Lanzavecchia and Sallusto, 2001), B cell activation in the follicle involves directed transport of antigen by diffusion or cell-mediated transport by B cells, macrophages, DCs, or follicular dendritic cells, depending on the size of the antigen (Batista and Harwood, 2009; Cyster, 2010). Within 1–3 days after initial antigen encounter, activated T and B cells migrate to the T-B zone border where they interact with each other (Vinuesa and Cyster, 2011). Activated B cells then differentiate into either short-lived antibody-secreting cells forming extrafollicular foci (MacLennan et al., 2003), or reenter the follicle to establish germinal centers (GCs), the hallmark of T-cell-dependent antibody responses (Gatto and Brink, 2010; Victora and Nussenzweig, 2012). In these anatomical structures, B cells undergo the processes of somatic hypermutation and affinity maturation, leading to the differentiation of memory B cells and long-lived plasma cells that produce high-affinity antibodies and eventually migrate to the bone marrow (Good-Jacobson and Shlomchik, 2010; Goodnow et al., 2010; McHeyzer-Williams et al., 2011; Tangye and Tarlinton, 2009).

T follicular helper cells (Tfh) have been described as a subset of $CD4^+$ T cells that are specialized in providing help to B cells, being crucial for the development and regulation of GCs and the establishment of serological memory (Crotty, 2011; King, 2009; McHeyzer-Williams et al., 2011; Vinuesa et al., 2010). Tfh cells are defined by their expression of the chemokine receptor CXCR5, which is required for migration toward the B cell follicle-derived chemokine CXCL13 (Ansel et al., 1999; Breitfeld et al., 2000; Kim et al., 2001; Schaerli et al., 2000). In addition, Tfh cells express the costimulatory molecules ICOS and PD-1 (Haynes et al., 2007), secrete the B cell-trophic cytokine IL-21 (Nurieva et al., 2008; Vogelzang et al., 2008), and are characterized by the expression of the transcriptional repressor *Bcl6* (Chtanova et al., 2004; Johnston et al., 2009; Nurieva et al., 2009; Yu et al., 2009). DCs can prime human naive T cells to differentiate into $CXCR5^+$ Tfh cells (Langenkamp et al., 2003; Ma et al., 2012), consistent with the finding in mice that BCL6 and CXCR5 can be induced in activated $CD4^+$ T cells in vivo in the absence of cognate interactions with B cells (Baumjohann et al., 2011; Choi et al., 2011; Goenka et al., 2011; Kerfoot et al., 2011; Kitano et al., 2011; Poholek et al., 2010). Nevertheless, B cells become the major antigen-presenting cell type for follicle-homing T cells at later stages of the immune response (Deenick et al., 2010; Haynes et al., 2007; Johnston et al., 2009; Glatman Zaretsky et al., 2009) and interactions with GC B cells might further polarize Tfh cells within the GC (Yusuf et al., 2010). Although intravital 2-photon microscopy studies have shown a dynamic behavior of Tfh cells in GCs (Allen et al., 2007; Hauser et al., 2007; Qi et al., 2008; Schwickert et al., 2007; Victora et al., 2010), how Tfh cells contribute to

the stability of GCs and how they are maintained themselves remains largely unknown. Here we showed that the amount of antigen dictates the Tfh cell and GC B cell response, and that maintenance of Tfh cells requires persistent antigen and GC B cells. We also showed that strong and prolonged Tfh cell responses can lead to bystander B cell activation, hypergammaglobulinemia, and production of poly- and self-reactive antibodies.

RESULTS

Tfh Cell and GC B Cell Numbers Are Highly Interrelated and Positively Correlate with the Amount of Available Antigen

In this study, we used classical adoptive transfer experiments in which low numbers of naive ovalbumin (OVA)-specific $CD4^+$ T cells from OT-II TCR-transgenic Rag-1-deficient mice were injected into wild-type (WT) C57BL/6 mice (OT-II→WT) or into *Cd3e*$^{-/-}$ mice (OT-II→*Cd3e*$^{-/-}$) that lack all T cells but have organized lymphoid organ structures and normal B cell development (Malissen et al., 1995). In both groups of mice, a rapid increase of OT-II cells was induced by intraperitoneal (i.p.) immunization with OVA (see Figure S1A available online). Three weeks after immunization, the number of OT-II cells declined in WT hosts, whereas it continued to increase, albeit to a lower extent, in *Cd3e*$^{-/-}$ hosts, most likely aided by the lymphopenic environment. OT-II cells recovered from both WT and *Cd3e*$^{-/-}$ mice were homogeneously $CD44^{hi}$ and a proportion of them stained positive for characteristic Tfh cell markers, including CXCR5, PD-1, ICOS, BTLA, and CD69 (data not shown). Ex vivo sorted $CXCR5^+$ OT-II cells expressed the Tfh cell transcription factor *Bcl6* and *Il21* (Figure S1B).

Using the above systems, we first analyzed the role of antigen dose on the expansion of OT-II cell numbers and on their differentiation into Tfh cells. OT-II→WT and OT-II→*Cd3e*$^{-/-}$ mice were immunized i.p. with increasing doses of OVA in adjuvants, and the spleen was analyzed on day +10 or day +14 by flow cytometry. In WT hosts there was a slight, albeit nonsignificant, increase in the total numbers of OT-II cells, whereas in *Cd3e*$^{-/-}$ hosts total OT-II cell numbers progressively increased with the dose of antigen administered (Figure 1A; Figure S1C). In both OT-II→WT and OT-II→*Cd3e*$^{-/-}$ mice, the percentage of Tfh cells (defined as $PD\text{-}1^+CXCR5^+$ or $ICOS^+CXCR5^+$) among OT-II cells was significantly higher with increased amounts of available antigen (Figure 1A; Figure S1C). The frequency of GC B cells (defined as $FAS^+GL\text{-}7^+$ B cells) also progressively increased with the dose of antigen administered (Figure 1B; Figure S1D). Plotting total numbers of OT-II Tfh and GC B cells of each individual mouse revealed a tight correlation between the two cell types (Figure 1C; Figure S1E). In WT hosts, the correlation was also observed for endogenous Tfh and GC B cells (data not shown). In *Cd3e*$^{-/-}$ hosts, the total number of Tfh cells was on average 5-fold higher than in WT hosts due to the larger expansion of OT-II cells in the lymphopenic environment. It should be noted that in *Cd3e*$^{-/-}$ hosts, OT-II cells did not vigorously proliferate and did not acquire a Tfh cell phenotype when the mice were immunized with a noncognate antigen, keyhole limpet hemocyanin (KLH)+MPL, or injected with PBS alone (Figure S1F).

Next, we analyzed the impact of chronic antigenic stimulation on the Tfh and GC B cell response. OT-II→WT mice were immunized with NP-OVA+alum to elicit a robust Tfh and GC B cell response; during the ensuing response, mice were injected with either PBS as a control (acute stimulation) or several doses of OVA protein in PBS (on day +4, +6, and +8, chronic stimulation) to provide a constant supply of antigen; the spleen was analyzed on day +9 by flow cytometry. Chronic antigenic stimulation led to a significant expansion of OT-II cells and to a large increase in the frequencies of $PD\text{-}1^+CXCR5^+$ Tfh cells and GC B cells as compared to mice that had received only a single NP-OVA+alum injection (Figure 1D). In chronic conditions, more than 50% of OT-II cells coexpressed PD-1 and CXCR5.

Taken together, the above results, obtained in different experimental systems, indicate that the magnitude of the Tfh and GC B cell response is dictated by the amount of available antigen and that Tfh and GC B cell numbers are highly interrelated.

Antigen Is Required to Maintain the Tfh Cell Phenotype

To assess whether sustained antigenic stimulation was required for the maintenance of Tfh cells, we used an adoptive transfer system in which $CD4^+$ TCR-tg T cells (SMARTA) specific for LCMV carry a heterozygous YFP-BCL6 reporter allele (Kitano et al., 2011) that allows for purification of viable $CXCR5^+BCL6^+$ Tfh cells. On day +4 following infection with LCMV, $CXCR5^+$ $YFP\text{-}BCL6^{hi}PD\text{-}1^{hi}$ Tfh and $CXCR5^-YFP\text{-}BCL6^{lo}PD\text{-}1^{int}$ non-Tfh SMARTA cells were isolated from primary hosts by cell sorting and retransferred into secondary hosts, which had been previously infected with LCMV or left untreated (Figure 2). In infected secondary recipients, most Tfh cells maintained their $PD\text{-}1^{hi}CXCR5^{hi}$ phenotype 2.5 days after retransfer. In contrast, Tfh cells strongly downregulated PD-1 and, to a lower extent, CXCR5 in noninfected mice (Figure 2). Interestingly, such a $PD\text{-}1^{lo}CXCR5^{int}$ phenotype has been recently correlated with central memory T (Tcm) cells that derived from a BCL6-dependent Tfh precursor population in a bacterial infection model (Pepper et al., 2011). Reciprocally, $YFP\text{-}CXCR5^-BCL6^{lo}PD\text{-}1^{lo}$ non-Tfh cells retained their phenotype in noninfected mice while a fraction acquired Tfh markers in infected mice (Figure 2). Thus, maintenance of the Tfh cell phenotype is dependent on sustained antigenic stimulation.

GC B Cells Are Required for the Maintenance of the Tfh Cell Phenotype

Although recent studies have demonstrated that DCs can prime naive T cells to differentiate into Tfh cells in the absence of cognate B cell interactions, B cells become the major antigen-presenting cell type for follicle-homing T cells at later stages of the immune response (Ma et al., 2012). We therefore set out to investigate the contribution of different B cell subsets in the maintenance of $PD\text{-}1^{hi}CXCR5^{hi}$ Tfh cells. To assess the role of follicular B cells versus GC B cells, we treated OT-II→WT mice with anti-CD20 on day +6 and day +8 after immunization in order to not interfere with the initial immune response and the establishment of GCs (Figure 3A). Anti-CD20 treatment significantly reduced total spleen cellularity and the number of $CD20^+CD19^+B220^+$ non-GC B cells (Figure 3B). In contrast, the number of GC B cells ($CD19^+B220^+FAS^+GL\text{-}7^+$) remained

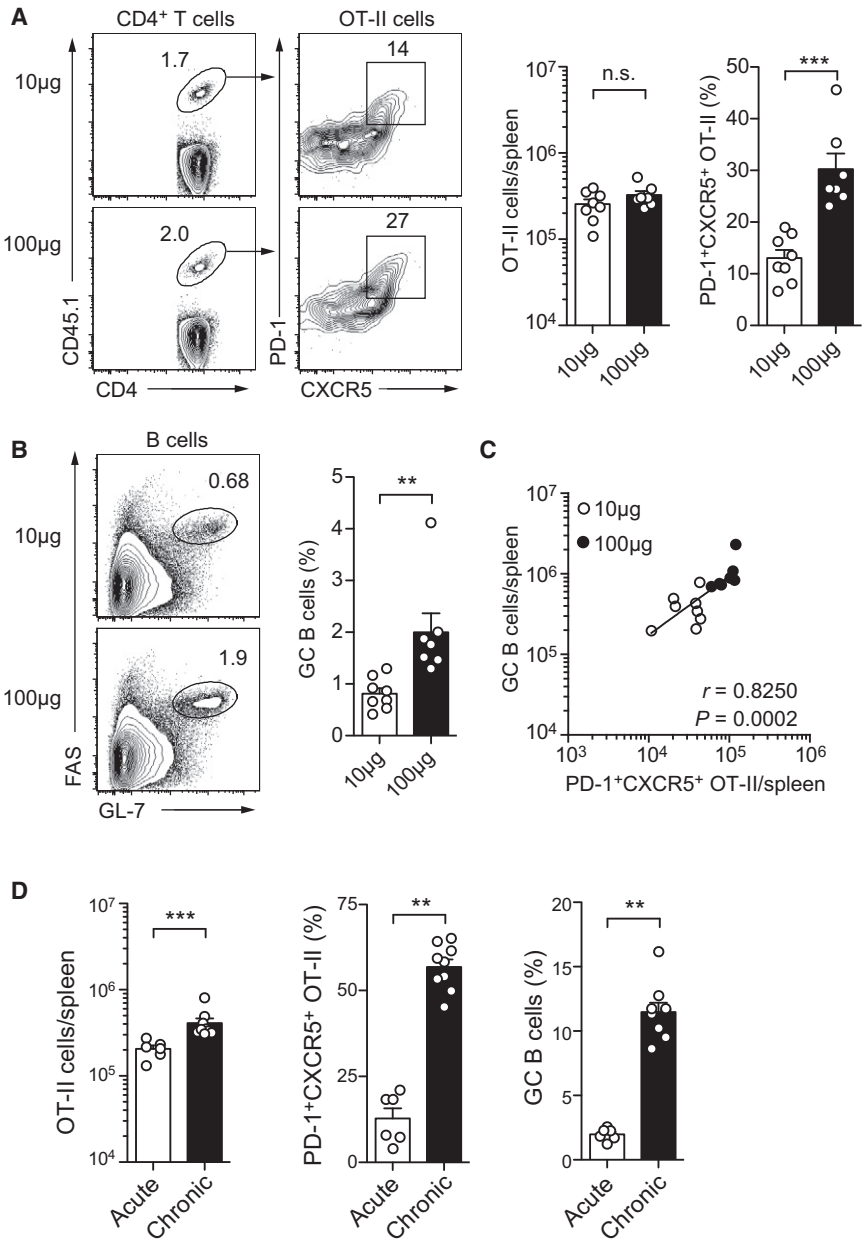

Figure 1. Tfh and GC B Cell Numbers Are Highly Interrelated and Positively Correlate with the Amount of Available Antigen

(A–C) Naive OT-II cells were adoptively transferred into WT mice and allowed to equilibrate in the host. Recipient mice were immunized intraperitoneally (i.p.) with 10 or 100 μg OVA in alum 16 hr later. Spleen cells were analyzed by flow cytometry on day +7 after immunization. (A) Representative contour plots show the percentage of CD45.1$^+$ OT-II cells among total CD4$^+$ T cells (7-AAD$^-$B220$^-$) and the percentage of PD-1^{hi}CXCR5^{hi} Tfh cells among the transferred OT-II cells. Total OT-II cell numbers and the frequency of OT-II Tfh cells are quantified in the bar graphs. Data are represented as mean ± SEM with each dot indicating one mouse (n = 7–8). (B) Representative contour plots show the percentage of FAS$^+$GL-7$^+$ GC B cells among total B cells (7AAD$^-$CD19$^+$B220$^+$). The frequency of GC B cells is quantified in the bar graph. Data are represented as mean ± SEM with each dot indicating one mouse (n = 7–8). (C) Graph shows the correlation between GC B cell and Tfh cell numbers. Data are representative of three independent experiments.

(D) Naive OT-II cells were adoptively transferred into WT hosts and all mice were immunized i.p. with NP-OVA in alum 16 hr later. One group of mice received additional injections of OVA in PBS without adjuvant on day +4, +6, and +8 (chronic, black bars), whereas the other group received only PBS (acute, white bars). On day +9, spleen cells were analyzed by flow cytometry for OT-II cell numbers, percentage of OT-II Tfh cells, and percentage of GC B cells. Gated on OT-II cells (7-AAD$^-$CD4$^+$CD45.1$^+$) or GC B cells (7-AAD$^-$CD19$^+$B220$^+$FAS$^+$GL-7$^+$). Data are represented as mean ± SEM with each dot indicating one mouse (n = 6–9). Data are representative of three independent experiments. See also Figure S1.

unchanged upon anti-CD20 treatment, a finding that is consistent with earlier reports (Gong et al., 2005). In addition, we did not observe an immediate effect on splenic plasma cell numbers (CD19^{int}B220^{lo}CD138^{hi}). Intriguingly, although the total number of OT-II cells was slightly reduced in the anti-CD20-treated animals, the percentage of OT-II cells with a Tfh cell phenotype was slightly, albeit not significantly, increased in mice treated with anti-CD20 antibody (Figure 3C). Thus, non-GC B cells appear to be dispensable for the maintenance of Tfh cells.

To address the role of GC B cells in the maintenance of Tfh cells, we took advantage of our observation that in mice expressing human diphtheria toxin receptor (DTR) and green fluorescent protein (GFP) under the control of the CD11c promoter (CD11c-DTR-GFP mice) (Jung et al., 2002), GFP was expressed not only in most DCs and in a fraction of plasma cells, as previously reported (Hebel et al., 2006; Jung et al., 2002; Probst et al., 2005), but also in a fraction (21% ± 2%) of GC B cells, whereas it was virtually absent in non-GC B cells (3.8% ± 0.2%) (Figure S2A). This surprising finding was further supported by the observation that GC B cells from immunized CD11c-YFP reporter mice (Lindquist et al., 2004) also had a high percentage of YFP$^+$ cells, as compared to marginal zone B cells and follicular B cells (Figure S2B).

To limit CD11c-DTR transgene expression to the B cell compartment, we generated mixed bone marrow (BM) chimeras by transferring bone-marrow cells from CD11c-DTR mice and B cell-deficient μMT mice into sublethally irradiated *Rag1*$^{-/-}$ hosts (Figure 4A). Thus, all B cells in this system were of CD11c-DTR donor origin, whereas DCs were of CD11c-DTR-negative donor and host origin. Eight weeks after reconstitution, BM-chimeric mice received naive OT-II cells and were

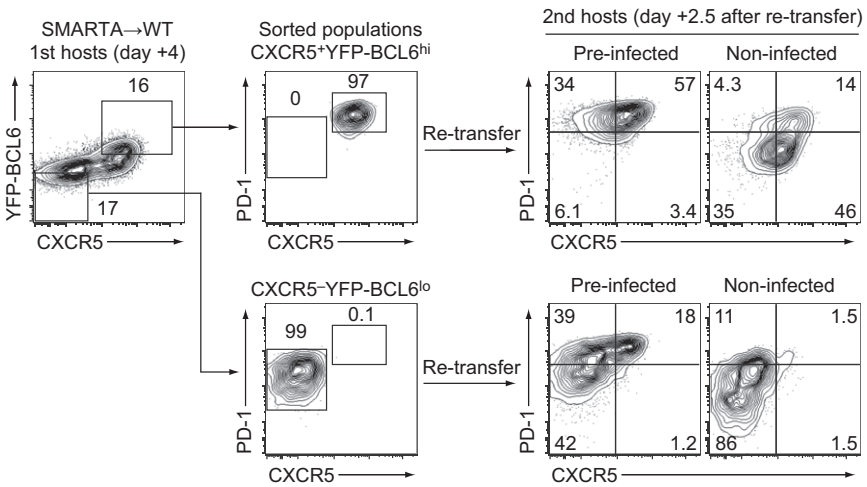

Figure 2. Sustained Antigenic Stimulation Is Required for the Maintenance of PD-1^{hi} CXCR5^{hi} Tfh Cells

Naive LCMV-specific SMARTA cells from CD45.1$^+$ *Bcl6*$^{yfp/+}$ reporter mice were adoptively transferred into naive WT mice. SMARTA Tfh (CXCR5$^+$YFP-BCL6$^+$PD-1^{hi}) and non- Tfh (CXCR5$^-$YFP-BCL6$^-$PD-1^{int}) cells were sorted from pooled spleens of primary recipient mice (n = 5) on day +4 after i.p. LCMV infection, and cells were retransferred into secondary hosts that were either naive or had been preinfected with LCMV 4 days before. After 2.5 days in the secondary recipients, retransferred SMARTA cells recovered from the spleens of the indicated mice were analyzed for their Tfh cell phenotype by flow cytometry. SMARTA cells were gated as 7AAD-CD45.1$^+$ CD4$^+$CD19$^-$ lymphocytes. Data are representative of two independent experiments.

challenged i.p. with NP-OVA+alum. Injection of diphtheria toxin (DTx) at the peak of the GC response (on day 6 and day 8) led to a strong reduction in total GC B cell numbers per spleen by day +9, whereas spleen cellularity, DC numbers, and non-GC B cell numbers were not affected by DTx treatment (Figure 4B). Importantly, the reduction of GC B cells was accompanied by a significant reduction in the frequency of Tfh cells (measured as either PD-1$^+$CXCR5$^+$ or ICOS$^+$CXCR5$^+$ T cells) in DTx-treated hosts, while total OT-II cell numbers were largely unaffected (Figure 4C). *Rag1*$^{-/-}$ mice reconstituted with CD11c-DTR-negative or WT bone marrow served as controls and did not show any alterations in cell numbers of the analyzed cell types upon DTx treatment (data not shown).

We also generated mixed BM chimeras by transferring BM cells from CD11c-DTR-*Cd3e*$^{-/-}$ and *Rag1*$^{-/-}$ donor mice into sublethally irradiated *Rag1*$^{-/-}$ hosts (Figure S2C). Reconstituted T cell-deficient hosts were injected with naive OT-II cells and challenged i.p. with NP-OVA+alum. Consistent with the results obtained in the T cell sufficient bone marrow chimeric mice, injection of DTx into CD11c-DTR-*Cd3e*$^{-/-}$→*Rag1*$^{-/-}$ chimeric mice at the peak of the GC response led to a strong reduction in total GC B cell numbers, which was accompanied by a significant reduction in the frequency of Tfh cells, whereas total OT-II cell numbers were largely unaffected (Figures S2D and S2E).

Taken together, these data indicate that the maintenance of Tfh cells is dependent on sustained cognate interactions with GC B cells.

ICOS:ICOS-L and CD40:CD40L Interactions Are Required for the Maintenance of Tfh Cells

To further characterize signaling pathways relevant to the maintenance of Tfh cells, we next sought to interfere with T cell-GC B cell interactions in vivo through administration of antibodies that block costimulatory signals. As in our previous experiments, antibodies were administered starting approximately 1 week after immunization in order to not interfere with the induction of robust GCs (Figure 5A). Treatment of immunized OT-II→WT mice with antibodies against ICOS-L (Figure 5B) or CD40L (Figure 5D) significantly reduced PD-1$^+$CXCR5$^+$ Tfh cell and FAS$^+$GL-7$^+$ GC B cell numbers. As seen before, there was a direct correlation between the number of Tfh cells and the number of GC B cells in individual mice that were either treated with blocking antibodies to ICOS-L or CD40L (Figures 5C and 5E). Blockade of ICOS:ICOS-L and CD40:CD40L interactions also led to a significant reduction of Tfh cell and GC B cell numbers in lymphopenic OT-II→*Cd3e*$^{-/-}$ mice (Figure S3). Taken together, these experiments indicate an important role for stimulatory ICOS:ICOS-L and CD40:CD40L interactions in the reciprocal maintenance of GC B cells and the Tfh cell phenotype during an established GC response.

Hypergammaglobulinemia and Polyreactive Antibodies in Immunized OT-II→*Cd3e*$^{-/-}$ Mice

As a functional readout of Tfh cells, we analyzed the antibody responses elicited by OVA immunization of OT-II→WT and OT-II→*Cd3e*$^{-/-}$ mice. Both groups of mice mounted a strong OVA-specific IgG response within the first 10 days after immunization with OVA+alum (821 ± 172 A.U. and 1192 ± 329 A.U., respectively, by day +10, Figure 6A). OVA-specific IgG antibodies remained at high amounts for several weeks afterward in OT-II→WT mice. In contrast, and in spite of the high numbers of Tfh cells (on average 5-fold higher than in WT hosts), OVA-specific IgG antibody amounts declined in OT-II→*Cd3e*$^{-/-}$ mice, reaching levels that were less than ¼ of that in OT-II→WT mice (675 ± 148 A.U. and 155 ± 49 A.U., respectively, by day +31). However, total serum IgG amounts increased rapidly in OT-II→*Cd3e*$^{-/-}$ mice and remained sustained for several weeks after immunization, reaching values higher than those in OT-II→WT mice (Figure 6B). The increase was most prominent for IgG1 and IgG2c, whereas IgG2b amounts were slightly increased and IgG3 amounts developed comparable to those measured in WT hosts. High amounts of total IgE were found in OT-II→*Cd3e*$^{-/-}$ mice, whereas this isotype was not detectable in WT hosts (Figure 6B). When compared to sera from OT-II→WT mice, the sera from immunized OT-II→*CD3e*$^{-/-}$ mice showed stronger nonspecific binding to ELISA plates (Figure 6C). In addition, antibodies to nuclear antigens (ANA) and ds-DNA could be detected in the sera from immunized OT-II→*CD3e*$^{-/-}$ mice but not from WT mice (Figures 6D and 6E), consistent with a fraction of these antibodies being "sticky" and self-reactive.

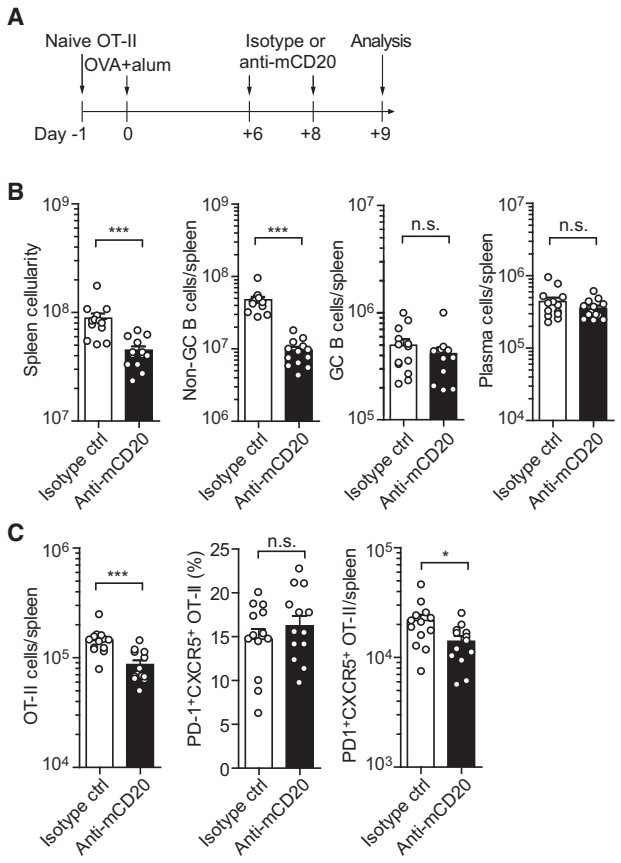

Figure 3. Non-GC B Cells Are Dispensable for the Maintenance of the Tfh Cell Phenotype

(A) Schematic outline of experimental approach: naive OT-II cells were adoptively transferred into WT mice and immunized i.p. with OVA+alum. Hosts were injected i.p. with 250 μg anti-murine CD20 antibody or anti-human CD20 antibody as isotype control on day +6 and +8. Spleens were dissected on day +9 and analyzed by flow cytometry.

(B) Spleen cellularity, non-GC B cell numbers (gated as 7-AAD$^-$CD19$^+$B220$^+$FAS$^-$GL-7$^-$), GC B cell numbers (7-AAD$^-$CD19$^+$B220$^+$FAS$^+$GL-7$^+$), and plasma cell numbers (7-AAD$^-$CD19^{int}B220^{lo}CD138^{hi}).

(C) OT-II cell numbers (7-AAD$^-$CD45.1$^+$CD4$^+$) as well as percentage and number of PD-1^{hi}CXCR5^{hi} OT-II cells. Data are represented as mean ± SEM (n = 13). Data are representative of four independent experiments.

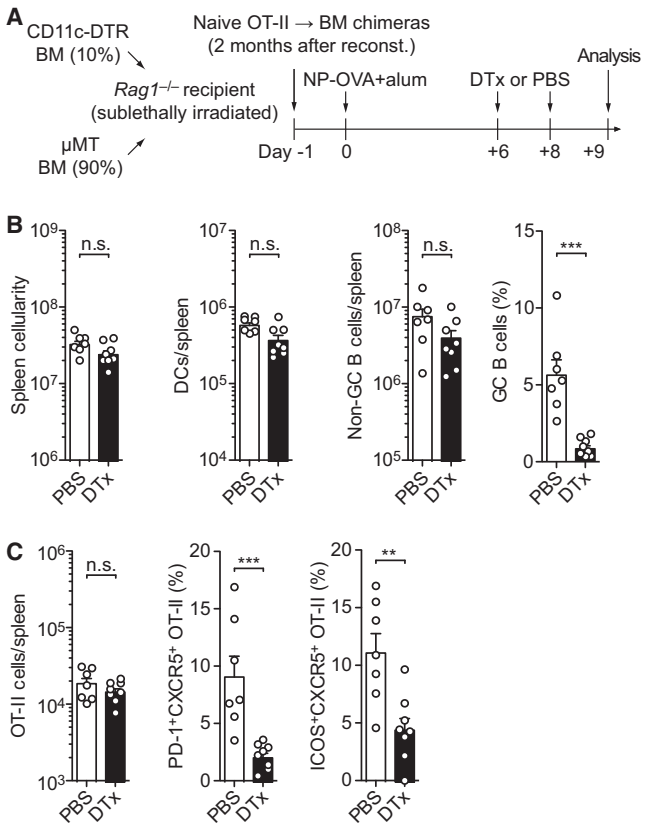

Figure 4. GC B Cells Are Required for the Maintenance of Tfh Cells

(A) Schematic outline of experimental approach: BM chimeras were generated by transferring 90% μMT and 10% CD11c-DTR bone-marrow cells into sublethally irradiated *Rag1*$^{-/-}$ hosts. Eight weeks later, naive OT-II cells were adoptively transferred into reconstituted hosts, followed by i.p. immunization with NP-OVA+alum. One group of mice received 4 ng DTx per gram of bodyweight on day +6 and +8, the other group received PBS only as control. Mice were sacrificed on day +9 and spleen cells were analyzed by flow cytometry for (B) total spleen cellularity, DC numbers (7-AAD$^-$CD19$^-$CD3ε$^-$CD11c^{hi}MHC-II^{hi}), non-GC B cell numbers (7-AAD$^-$CD19$^+$B220$^+$FAS$^-$GL-7$^-$), and percentage of GC B cells (7-AAD$^-$CD19$^+$B220$^+$FAS$^+$GL-7$^+$).

(C) Total OT-II cell numbers as well as percentages of PD-1$^+$CXCR5$^+$ and ICOS$^+$CXCR5$^+$ OT-II Tfh cells. Data shown are mean ± SEM (n = 7–8 mice). Data are representative of five independent experiments. See also Figure S2.

The increase in total IgG observed in lymphopenic *CD3e*$^{-/-}$ hosts would be consistent with activation of B cells of irrelevant specificity by the large numbers of OT-II Tfh cells. To provide direct evidence for this phenomenon, we transferred OT-II cells together with polyclonal B cells carrying a congenic marker into SW$_{HEL}$-*Rag1*$^{-/-}$ host mice (all B cells specific for HEL) and immunized the recipients with OVA+alum. As expected, a fraction of the transferred polyclonal B cells became activated and acquired a GC phenotype (Figure S4). Strikingly, also a fraction of endogenous HEL-specific B cells became activated, acquired a GC phenotype and produced class-switched IgG1 antibodies (Figure S4).

Taken together, these results indicate that in lymphopenic conditions Tfh cells can provide help to bystander B cells and drive them into the GC reaction, thus leading to the production of isotype-switched antibodies of irrelevant specificities, including poly-reactive and self-reactive antibodies.

DISCUSSION

In this study, we report several important findings. First, the magnitude of the Tfh response is dictated by the amount of antigen and directly correlates with the number of GC B cells. Second, the Tfh cell phenotype is dependent on sustained antigenic stimulation, as shown by the rapid loss of PD-1 and high CXCR5 expression upon transfer into antigen-naive recipients. Third, and more importantly, maintenance of Tfh cells during the GC reaction requires sustained interaction with GC B cells. This conclusion is supported by the dramatic reduction in Tfh cell numbers upon selective depletion of GC B cells,

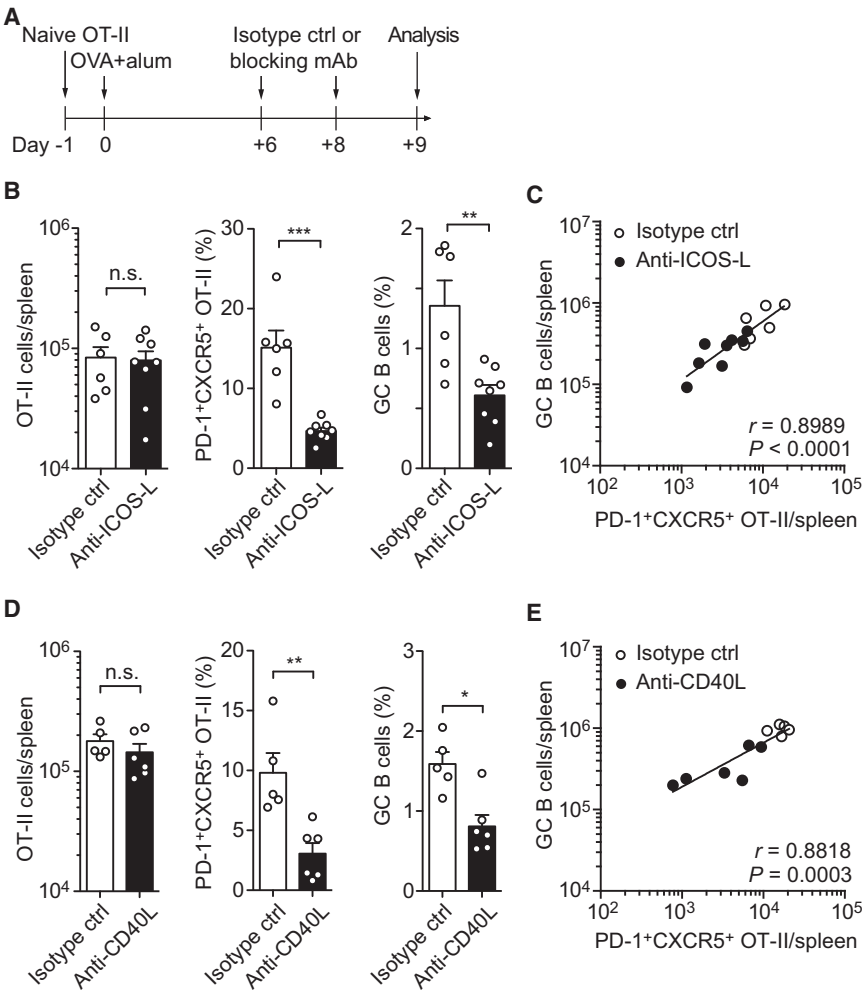

Figure 5. ICOS:ICOS-L and CD40:CD40L Interactions Are Required for the Maintenance of Mature Tfh Cells

(A) Schematic outline of experimental approach: naive OT-II cells were adoptively transferred into WT mice and immunized i.p. with OVA+alum. Hosts were injected i.p. with blocking antibodies or appropriate isotype controls starting around 1 week after immunization in order to not interfere with initial priming of T cells and establishment of GCs.

(B and C) Anti-iCOS-L (clone HK5.3) or appropriate isotype control antibodies (250 μg per mouse) were injected into OT-II→WT mice on day +6 and +8 after immunization, and spleens were analyzed by flow cytometry on day +9. (B) shows OT-II cell numbers (7-AAD$^-$CD45.1$^+$CD4$^+$), percentage of PD-1$^+$CXCR5$^+$ OT-II Tfh cells, and percentage of GC B cells (7-AAD$^-$CD19$^+$B220$^+$FAS$^+$GL-7$^+$). Data are represented as mean ± SEM (n = 5–8). (C) Graph shows the correlation between GC B cell and OT-II Tfh cell numbers. Data are representative of three independent experiments.

(D and E) Anti-CD40L (clone HK5.3) or appropriate isotype control antibodies (200 μg per mouse) were injected on day +6 and +8 after immunization. Spleens were dissected on day +9 and analyzed by flow cytometry as in (B) and (C). Data are represented as mean ± SEM (n = 5–6) and are representative of three independent experiments. See also Figure S3.

but not of non-GC B cells. The reduction of Tfh cell numbers upon blockade of costimulatory pathways such as CD40:CD40L and ICOS:ICOS-L in established GCs and the strong correlation between Tfh and GC B cell numbers further highlight a tight regulation between Tfh cells and GC B cells.

There is an ongoing debate whether Tfh cells represent a separate Th cell lineage or a transient activation state (Crotty, 2011; Fazilleau et al., 2009; King, 2009). Our findings provide strong evidence that the Tfh cell phenotype is of a transient nature. They also reveal a substantial difference between Tfh cells and other differentiated Th cells, such as Th1 and Th2 cells, which can be maintained in the absence of antigen and polarizing cytokines (O'Shea and Paul, 2010). Interestingly, the PD-1$^+$CXCR5$^+$ cells that have lost their Tfh phenotype upon transfer into antigen-free hosts still maintained intermediate levels of CXCR5, a phenotype that has been recently attributed to Tcm cells (Pepper et al., 2011) and that may correspond to human circulating Tfh cells (Breitfeld et al., 2000).

The finding that the Tfh cell phenotype is critically dependent on sustained antigenic stimulation could explain recent observations that viral persistence preferentially directs Tfh cell generation in a model of chronic LCMV infection (Fahey et al., 2011) and that Foxp3$^+$ Treg cells convert into Tfh cells in Peyer's patches of lymphopenic *CD3e*$^{-/-}$ hosts (Tsuji et al., 2009). In the latter study, Foxp3$^+$ Treg cells only converted into Tfh cells in the gut, but not in spleen and lymph nodes, an observation that was attributed to the availability of certain Tfh cell-inducing cytokines, such as IL-6 (Tsuji et al., 2009). Given that the Foxp3$^+$ Treg cells were transferred into nonimmunized *CD3e*$^{-/-}$ recipients, it is likely that the availability of gut antigens, and thus sustained TCR stimulation, together with the abundant proinflammatory signals, drove the preferential development of Tfh cells from Foxp3$^+$ Treg cells in gut Peyer's patches.

Whether a sustained presence of Tfh cells in GC is beneficial for the immune response remains to be established. Previous studies have shown that strong virus-specific CD4$^+$ T cell activation results in heightened polyclonal B cell activation, which competes with virus-specific B cell activation and the formation of neutralizing antibodies (Recher et al., 2004). As in the case of these early reports, the bystander B cell activation that we have observed in the present study seems to be the consequence of the large numbers of highly stimulatory Tfh cells that develop in lymphopenic mice. In conditions of polyclonal B cell activation, cognate CD4$^+$ T cell-B cell interactions may be less efficient because antigen-specific B cells and plasma cells have to compete for survival factors in lymphoid organs or in the bone marrow, thus explaining the curtailed OVA-specific response. Recent studies provided evidence for a follicular CD4$^+$ Treg cell population (defined as Tfr cell) that shares characteristics

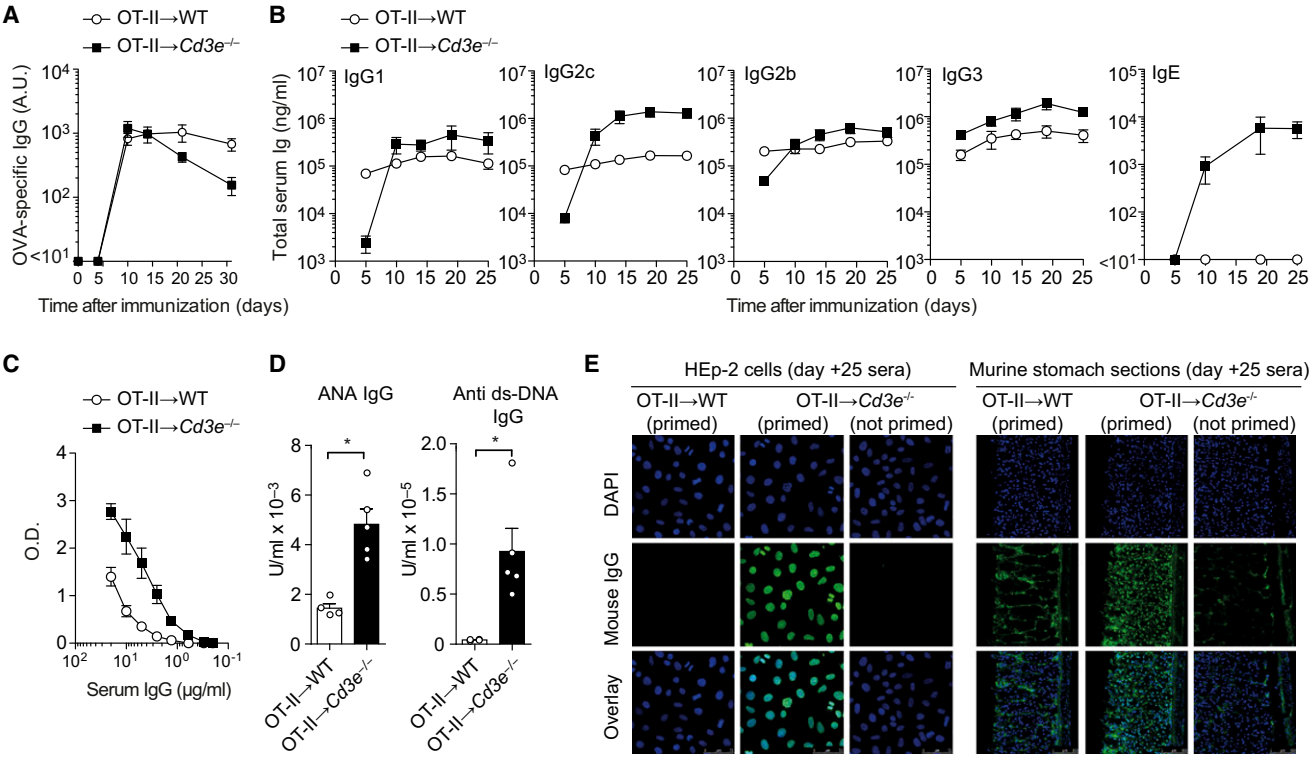

Figure 6. Bystander B Cell Activation, Hypergammaglobulinemia, and Production of Poly- and Self-Reactive Antibodies in Immunized OT-II→*Cd3e*$^{-/-}$ Mice

(A and B) OT-II→WT and OT-II→*Cd3e*$^{-/-}$ mice were immunized i.p. with OVA+alum. Serum was collected at the indicated time points after immunization, and OVA-specific IgG (A) or total Ig of the indicated isotypes (B) were measured by ELISA. Data are represented as mean ± SEM (n = 4–5).

(C) Total serum IgG was measured by ELISA from samples collected on day 28 and different IgG concentrations were applied to uncoated, BSA-blocked ELISA plates. Bound IgG antibody levels were determined by ELISA. O.D. values are shown as mean ± SEM (n = 5).

(D) Anti-nuclear antibodies (ANA) and anti ds-DNA antibodies were measured in the sera of day +25 OT-II→WT and OT-II→*Cd3e*$^{-/-}$ immunized mice. Data are represented as mean ± SEM (n = 4–5).

(E) Sera (1:1,000) from day +25 OT-II→WT and OT-II→*Cd3e*$^{-/-}$ immunized mice (primed) or OT-II→*Cd3e*$^{-/-}$ mice immunized with PBS+alum (not primed) were analyzed for the presence of ANA by incubation on HEp-2 slides or murine stomach sections. Mouse IgG ANA were detected by Alexa Fluor-488 goat anti-mouse IgG F(ab)$_2$ fragments. Nuclei were counterstained with DAPI. Data are representative of three independent experiments that yielded similar results. See also Figure S4.

of natural Treg and Tfh cells and restrains excessive Tfh and GC B cell responses (Alexander et al., 2011; Chung et al., 2011; Linterman et al., 2011; Wollenberg et al., 2011). Further studies will be required to address the role of Tfr cells or other T cell populations in the dysregulated antibody response observed in lymphopenic mice.

One interesting finding of our study is that CD11c-DTR transgene expression by GC B cells rendered these cells highly susceptible to DTx-mediated depletion. Several authors have cautioned that the relatively broad expression of CD11c makes it essential to carefully plan and interpret experiments that make use of CD11c reporter mice (Murphy, 2011; Probst et al., 2005). Thus, we took special care to generate BM chimeras with restricted CD11c-DTR expression within the B cell lineage. It should be noted that not all GC B cells stained positive for GFP or YFP in the two different mouse strains used for these experiments. We speculate that CD11c might be expressed at different stages in the life of GC B cells, for instance during their passage through the dark or light zones. Nevertheless, GC B cell depletion by this method was highly selective and resulted in a remarkable reduction in both GC B cell and Tfh cell numbers. Future experiments should be aimed at further dissecting the precise kinetics of CD11c expression in GC B cells.

Besides their well-established role in driving antibody production, Tfh cells are emerging as central intermediaries of other T helper cell-mediated immune responses. Tfh-like transitions of activated T cells have been correlated with Th1 effector cell differentiation (Nakayamada et al., 2011; Oestreich et al., 2012) and also with the generation of cells with a Tcm phenotype (Pepper et al., 2011). Interestingly, although anti-CD20 treatment has been shown to ameliorate disease severity in several autoimmune diseases, such as in multiple sclerosis (Hauser et al., 2008), it does not necessarily reduce autoantibody levels in these patients. Given that GC B cells are only inefficiently depleted by anti-CD20 treatment, it may be possible that the anti-CD20 treatment selectively interferes with early T cell-B cell interactions involved in Th1 and Tcm cell generation, whereas established Tfh cells could remain an important driver of autoimmune progression in this situation.

In conclusion, our data identify antigen-presenting cells and costimulatory molecules that are required for the maintenance of Tfh cells and suggest a link between overwhelming Tfh cell responses and the development of dysregulated humoral immune responses. These data are not only relevant in the context of emerging models of Tfh cell development and function but also suggest that therapies aiming at specifically disrupting Tfh cell-GC B cell interactions may be useful in the treatment of antibody-mediated autoimmune diseases, such as rheumatoid arthritis and systemic lupus erythematosus. Furthermore, our findings may have implications for the treatment of patients with congenital defects in lymphocyte homeostasis and patients suffering from diseases involving lymphopenia, such as HIV infection (Lindqvist et al., 2012) or certain tumors.

EXPERIMENTAL PROCEDURES

Mice

SMARTA (Oxenius et al., 1998), SW_{HEL} (Phan et al., 2003), and YFP-BCL6 (Kitano et al., 2011) mice have been described previously. OT-II (004194), μMT (002288), CD11c-DTR (004509), CD11c-YFP (008829), and *Rag1*$^{-/-}$ (002216) mice were obtained from The Jackson Laboratory. *Cd3e*$^{-/-}$ mice, which lack all T cells but have organized lymphoid organ structures and normal B cell development, have been described previously (Malissen et al., 1995). These mice have basal serum IgM levels comparable to WT mice but lack IgG1, have reduced levels of IgG2b, IgG2c, and IgA, and increased levels of IgG3 (data not shown). All OT-II donor mice were bred and maintained on a *Rag1*$^{-/-}$ background. SMARTA mice were maintained on a WT background. For identification of transferred cells within hosts, donor mice were bred onto homo- or heterozygous CD45.1 allele backgrounds. For B cell-specific CD11c-DTR BM-chimeras, 90% bone-marrow cells from μMT or *Rag1*$^{-/-}$ donors and 10% bone marrow cells from CD11c-DTR donors were transferred into sublethally irradiated *Rag1*$^{-/-}$ hosts. Chimeras were used 2 months after successful reconstitution. All mice were bred and maintained under specific pathogen-free conditions. Animals were treated in accordance with guidelines of the Swiss Federal Veterinary Office or the Institutional Animal Care and Use Committee guidelines of the University of California, San Francisco, and experiments were approved by the Dipartimento della Sanità e Socialità of Canton Ticino.

Adoptive Cell Transfers

Single-cell suspensions were prepared by mincing spleens and peripheral lymph nodes between the frosted ends of glass slides, and cell suspensions were filtered through fine mesh. CD4$^+$ T cells were first enriched with the Naive T Cell Isolation Kit (Miltenyi Biotec) or by positive selection with anti-CD4-FITC antibodies (clone RM4-5) followed by anti-FITC microbeads (Miltenyi Biotec). Naive CD4$^+$CD8$^-$CD44^{lo}CD62L^{hi}CD25$^-$ T cells were then sorted on a FACSAria cell sorter (BD Biosciences) to >99% purity. Low numbers of OT-II cells (1–5 × 10^4 cells per mouse) were injected intravenously (i.v.) and allowed to equilibrate within the host for 16–24 hr before immunization. For infection experiments, 1 × 10^6 naive SMARTA cells from *Bcl6*$^{yfp/+}$ reporter mice were transferred into congenic primary recipients, followed by i.p. infection with LCMV the next day. CD45.1$^+$ Tfh (CXCR5$^+$YFP-BCL6^{hi}) and non-Tfh (CXCR5$^-$YFP-BCL6^{lo}) SMARTA cell populations were sorted from the pooled spleens on day +4 and retransferred into secondary hosts that had been preinfected with LCMV 4 days before or left untreated and all hosts were analyzed 2.5 days later.

Immunizations, Infections, and Diphtheria Toxin Treatment

Mice were immunized intraperitoneally with endotoxin-free, >98% purity OVA (Endograde OVA; Profos), KLH (Calbiochem), NP-OVA, or NP-KLH (Biosearch Technologies), in combination with 10 μg monophosphoryl lipid A (Sigma-Aldrich) or Imject Alum (Pierce Biotechnology) as adjuvants. For viral infections, mice were injected i.p. with 2 × 10^6 PFU LCMV Armstrong strain. For depletion of CD11c-DTR-sensitive cells, diphtheria toxin from Corynebacterium diphtheriae (Sigma-Aldrich) was diluted in 200 μl PBS according to the weight of the mice (4 ng per kg of body weight) and injected i.p.

In Vivo Antibody Treatments

Anti-CD40L (hamster IgG, clone MR-1), anti-iCOS-L (rat IgG2a, clone HK5.3; with permission from Hideo Yagita), and appropriate isotype controls were purchased from Bio X Cell. Anti-mouse CD20 (mouse IgG1, clone 18B12) and anti-human CD20 (mouse IgG1, clone 2B8, used as isotype control) antibodies were kindly provided by Robert Dunn (Biogen Idec). Recipient mice were injected i.p. with 200–250 μg of respective antibodies in PBS every 2 days starting approximately 1 week after immunization in order to not interfere with the initiation of GCs. If not otherwise stated, flow cytometric analyses were usually performed on day +9 after immunization.

Flow Cytometry

The following antibodies or streptavidin, conjugated to biotin, FITC, Alexa Fluor (AF) 488, PE, PE-Cy7, PerCP-Cy5.5, APC, AF647, APC-Cy7, APC-AF750, APC-H7, Pacific Blue, eFluor450, Qdot605, or Pacific Orange were purchased from BD Biosciences, eBioscience, Biolegend, or Invitrogen: CD3ε (clone 145-2C11), CD4 (RM4-5), CD8α (53-6.7), CD11c (N418), CD19 (1D3), CD25 (7D4), CD28 (37.51), CD62L (MEL-14), CD44 (IM7), CD45.1 (A20), CD45.2 (104), PD-1 (RMP1-30 or J43), B220 (RA3-6B2), FAS (Jo2), GL-7, IgD (11-26c), CD21 (7E9), CD23 (B3B4), MHC class II (M5/114.15.2), and CXCR5 (2G8). PNA was used either conjugated to AF647 (Invitrogen) or to biotin (Vector Laboratories). Dead cells were excluded with 7-AAD (eBioscience). In some experiments, certain cell types were excluded in a dump channel with PerCP-conjugated anti-CD4, CD8, CD11b, Gr-1, F4/80, and/or B220. Routine 7- to 8-color flow cytometry was performed on a FACSCanto II or LSR II (BD Biosciences) and data were evaluated using FlowJo software (TriStar).

Quantitative Real-Time PCR

Transferred OT-II T cells were enriched from the spleen of recipient mice using anti-CD45.1-FITC antibodies and anti-FITC microbeads (Miltenyi Biotec) and further sorted by FACS into CXCR5$^+$ and CXCR5$^-$ cell fractions. RNA was prepared using TRIzol LS reagent (Invitrogen), transcribed into cDNA, and analyzed as described before (Reboldi et al., 2009).

ELISA

ELISA was performed as previously described (Kingston et al., 2009). In brief, 96-well half-area plates (Costar) were coated overnight with 5 μg/ml anti-ig antibodies or 10μg/ml antigen in PBS at 4°C. Plates were blocked with 1% BSA/PBS, and serial dilutions of sera in 1% BSA/PBS were applied to the plates and incubated at RT. Alkaline phosphatase-conjugated anti-mouse Ig isotype-specific antibodies (Southern Biotechnologies) followed by pNPP substrate (Sigma-Aldrich) were used as detection reagents. Absorbance was measured at 405 nm with a microplate reader (Molecular Devices) and absolute values were calculated according to Ig standards (Southern Biotechnologies) or reference serum from hyperimmunized mice (expressed in arbitrary units, AU). IgE levels were measured with rat anti-mouse IgE (clone R35-118) as capture antibody and biotinylated rat anti-mouse IgE (clone R35-72) as detection antibody (both from BD Biosciences), followed by avidin-HRP (Sigma-Aldrich) and ABTS according to the manufacturer's instructions.

Autoantibody Detection

Commercially available HEp-2 and mouse tissue slides (Orgentec) were used for the detection of autoantibodies in the sera of immunized mice with AF488-conjugated goat anti-mouse IgG $F(ab)_2$ fragments (Invitrogen). Nuclei were counterstained with DAPI (Sigma). Images were acquired on a confocal Leica TS5 system. Images were processed with Photoshop (Adobe) software without nonlinear operations. Anti-dsDNA and ANA IgG were determined using commercial kits from Alpha Diagnostic according to the manufacturer's instructions.

Statistics

Data were analyzed with Prism 5 (GraphPad Software) using the two-tailed nonparametric Mann-Whitney U test. Graphs show the mean ± SEM.

*, $p < 0.05$; **, $p < 0.01$; ***, $p < 0.001$. The correlation coefficient r and the respective p value were also calculated with Prism 5.

SUPPLEMENTAL INFORMATION

Supplemental Information includes four figures and can be found with this article online at http://dx.doi.org/10.1016/j.immuni.2012.11.020.

ACKNOWLEDGMENTS

The authors would like to thank Takaharu Okada (RIKEN) for YFP-BCL6 mice; Robert Brink (Garvan Institute) for providing SW_{HEL} mice through Antonio Freitas (Institut Pasteur); Hideo Yagita for the anti-iCOS-L antibodies; Robert Dunn (Biogen Idec) for the anti-CD20 antibodies; Mehrdad Matloubian (UCSF) for LCMV; David Jarrossay for cell sorting; Luana Perlini, Enrica Mira Catô, Andrea D'Ercole, and Emanuele Cavadini for technical support and animal care; and Dior Baumjohann, Afonso Almeida, and Chris Allen for insightful discussions. D.B. designed and performed experiments, analyzed and interpreted data, and wrote the manuscript; S.P. performed and analyzed experiments; A.R. and F.R. performed some of the experiments; K.M.A. provided vital reagents and intellectual input; A.L. conceived of the project and wrote the manuscript; F.S. conceived of the project, wrote the manuscript, and provided overall direction of the study. S.P. conducted this study as partial fulfillment of her PhD in Molecular Medicine, Program in Basic and Applied Immunology, San Raffaele University, Milan, Italy. This work was supported by a Boehringer Ingelheim Fonds PhD Scholarship and a Swiss National Science Foundation Postdoctoral Fellowship (to D.B.), and by grants from the Swiss National Science Foundation (N. 116440 and 131092 to F.S. and 126027 to A.L.). The Institute for Research in Biomedicine is supported by the Helmut Horten Foundation.

Received: September 29, 2011
Accepted: November 12, 2012
Published: March 14, 2013

REFERENCES

Alexander, C.M., Tygrett, L.T., Boyden, A.W., Wolniak, K.L., Legge, K.L., and Waldschmidt, T.J. (2011). T regulatory cells participate in the control of germinal centre reactions. Immunology *133*, 452–468.

Allen, C.D., Okada, T., Tang, H.L., and Cyster, J.G. (2007). Imaging of germinal center selection events during affinity maturation. Science *315*, 528–531.

Ansel, K.M., McHeyzer-Williams, L.J., Ngo, V.N., McHeyzer-Williams, M.G., and Cyster, J.G. (1999). In vivo-activated CD4 T cells upregulate CXC chemokine receptor 5 and reprogram their response to lymphoid chemokines. J. Exp. Med. *190*, 1123–1134.

Batista, F.D., and Harwood, N.E. (2009). The who, how and where of antigen presentation to B cells. Nat. Rev. Immunol. *9*, 15–27.

Baumjohann, D., Okada, T., and Ansel, K.M. (2011). Cutting Edge: Distinct waves of BCL6 expression during T follicular helper cell development. J. Immunol. *187*, 2089–2092.

Breitfeld, D., Ohl, L., Kremmer, E., Ellwart, J., Sallusto, F., Lipp, M., and Förster, R. (2000). Follicular B helper T cells express CXC chemokine receptor 5, localize to B cell follicles, and support immunoglobulin production. J. Exp. Med. *192*, 1545–1552.

Choi, Y.S., Kageyama, R., Eto, D., Escobar, T.C., Johnston, R.J., Monticelli, L., Lao, C., and Crotty, S. (2011). ICOS receptor instructs T follicular helper cell versus effector cell differentiation via induction of the transcriptional repressor Bcl6. Immunity *34*, 932–946.

Chtanova, T., Tangye, S.G., Newton, R., Frank, N., Hodge, M.R., Rolph, M.S., and Mackay, C.R. (2004). T follicular helper cells express a distinctive transcriptional profile, reflecting their role as non-Th1/Th2 effector cells that provide help for B cells. J. Immunol. *173*, 68–78.

Chung, Y., Tanaka, S., Chu, F., Nurieva, R.I., Martinez, G.J., Rawal, S., Wang, Y.H., Lim, H., Reynolds, J.M., Zhou, X.H., et al. (2011). Follicular regulatory T cells expressing Foxp3 and Bcl-6 suppress germinal center reactions. Nat. Med. *17*, 983–988.

Crotty, S. (2011). Follicular helper CD4 T cells (TFH). Annu. Rev. Immunol. *29*, 621–663.

Cyster, J.G. (2010). B cell follicles and antigen encounters of the third kind. Nat. Immunol. *11*, 989–996.

Deenick, E.K., Chan, A., Ma, C.S., Gatto, D., Schwartzberg, P.L., Brink, R., and Tangye, S.G. (2010). Follicular helper T cell differentiation requires continuous antigen presentation that is independent of unique B cell signaling. Immunity *33*, 241–253.

Fahey, L.M., Wilson, E.B., Elsaesser, H., Fistonich, C.D., McGavern, D.B., and Brooks, D.G. (2011). Viral persistence redirects CD4 T cell differentiation toward T follicular helper cells. J. Exp. Med. *208*, 987–999.

Fazilleau, N., Mark, L., McHeyzer-Williams, L.J., and McHeyzer-Williams, M.G. (2009). Follicular helper T cells: lineage and location. Immunity *30*, 324–335.

Gatto, D., and Brink, R. (2010). The germinal center reaction. J Allergy Clin Immunol *126*, 898–907, quiz 908-899.

Glatman Zaretsky, A., Taylor, J.J., King, I.L., Marshall, F.A., Mohrs, M., and Pearce, E.J. (2009). T follicular helper cells differentiate from Th2 cells in response to helminth antigens. J. Exp. Med. *206*, 991–999.

Goenka, R., Barnett, L.G., Silver, J.S., O'Neill, P.J., Hunter, C.A., Cancro, M.P., and Laufer, T.M. (2011). Cutting edge: dendritic cell-restricted antigen presentation initiates the follicular helper T cell program but cannot complete ultimate effector differentiation. J. Immunol. *187*, 1091–1095.

Gong, Q., Ou, Q., Ye, S., Lee, W.P., Cornelius, J., Diehl, L., Lin, W.Y., Hu, Z., Lu, Y., Chen, Y., et al. (2005). Importance of cellular microenvironment and circulatory dynamics in B cell immunotherapy. J. Immunol. *174*, 817–826.

Good-Jacobson, K.L., and Shlomchik, M.J. (2010). Plasticity and heterogeneity in the generation of memory B cells and long-lived plasma cells: the influence of germinal center interactions and dynamics. J. Immunol. *185*, 3117–3125.

Goodnow, C.C., Vinuesa, C.G., Randall, K.L., Mackay, F., and Brink, R. (2010). Control systems and decision making for antibody production. Nat. Immunol. *11*, 681–688.

Hauser, A.E., Junt, T., Mempel, T.R., Sneddon, M.W., Kleinstein, S.H., Henrickson, S.E., von Andrian, U.H., Shlomchik, M.J., and Haberman, A.M. (2007). Definition of germinal-center B cell migration in vivo reveals predominant intrazonal circulation patterns. Immunity *26*, 655–667.

Hauser, S.L., Waubant, E., Arnold, D.L., Vollmer, T., Antel, J., Fox, R.J., Bar-Or, A., Panzara, M., Sarkar, N., Agarwal, S., et al.; HERMES Trial Group. (2008). B-cell depletion with rituximab in relapsing-remitting multiple sclerosis. N. Engl. J. Med. *358*, 676–688.

Haynes, N.M., Allen, C.D., Lesley, R., Ansel, K.M., Killeen, N., and Cyster, J.G. (2007). Role of CXCR5 and CCR7 in follicular Th cell positioning and appearance of a programmed cell death gene-1high germinal center-associated subpopulation. J. Immunol. *179*, 5099–5108.

Hebel, K., Griewank, K., Inamine, A., Chang, H.D., Müller-Hilke, B., Fillatreau, S., Manz, R.A., Radbruch, A., and Jung, S. (2006). Plasma cell differentiation in T-independent type 2 immune responses is independent of CD11c(high) dendritic cells. Eur. J. Immunol. *36*, 2912–2919.

Johnston, R.J., Poholek, A.C., DiToro, D., Yusuf, I., Eto, D., Barnett, B., Dent, A.L., Craft, J., and Crotty, S. (2009). Bcl6 and Blimp-1 are reciprocal and antagonistic regulators of T follicular helper cell differentiation. Science *325*, 1006–1010.

Jung, S., Unutmaz, D., Wong, P., Sano, G., De los Santos, K., Sparwasser, T., Wu, S., Vuthoori, S., Ko, K., Zavala, F., et al. (2002). In vivo depletion of CD11c+ dendritic cells abrogates priming of CD8+ T cells by exogenous cell-associated antigens. Immunity *17*, 211–220.

Kerfoot, S.M., Yaari, G., Patel, J.R., Johnson, K.L., Gonzalez, D.G., Kleinstein, S.H., and Haberman, A.M. (2011). Germinal center B cell and T follicular helper cell development initiates in the interfollicular zone. Immunity *34*, 947–960.

Kim, C.H., Rott, L.S., Clark-Lewis, I., Campbell, D.J., Wu, L., and Butcher, E.C. (2001). Subspecialization of CXCR5+ T cells: B helper activity is focused in

a germinal center-localized subset of CXCR5+ T cells. J. Exp. Med. *193*, 1373–1381.

King, C. (2009). New insights into the differentiation and function of T follicular helper cells. Nat. Rev. Immunol. *9*, 757–766.

Kingston, D., Schmid, M.A., Onai, N., Obata-Onai, A., Baumjohann, D., and Manz, M.G. (2009). The concerted action of GM-CSF and Flt3-ligand on in vivo dendritic cell homeostasis. Blood *114*, 835–843.

Kitano, M., Moriyama, S., Ando, Y., Hikida, M., Mori, Y., Kurosaki, T., and Okada, T. (2011). Bcl6 protein expression shapes pre-germinal center B cell dynamics and follicular helper T cell heterogeneity. Immunity *34*, 961–972.

Langenkamp, A., Nagata, K., Murphy, K., Wu, L., Lanzavecchia, A., and Sallusto, F. (2003). Kinetics and expression patterns of chemokine receptors in human CD4+ T lymphocytes primed by myeloid or plasmacytoid dendritic cells. Eur. J. Immunol. *33*, 474–482.

Lanzavecchia, A., and Sallusto, F. (2001). Regulation of T cell immunity by dendritic cells. Cell *106*, 263–266.

Lindquist, R.L., Shakhar, G., Dudziak, D., Wardemann, H., Eisenreich, T., Dustin, M.L., and Nussenzweig, M.C. (2004). Visualizing dendritic cell networks in vivo. Nat. Immunol. *5*, 1243–1250.

Lindqvist, M., van Lunzen, J., Soghoian, D.Z., Kuhl, B.D., Ranasinghe, S., Kranias, G., Flanders, M.D., Cutler, S., Yudanin, N., Muller, M.I., et al. (2012). Expansion of HIV-specific T follicular helper cells in chronic HIV infection. J. Clin. Invest. *122*, 3271–3280.

Linterman, M.A., Pierson, W., Lee, S.K., Kallies, A., Kawamoto, S., Rayner, T.F., Srivastava, M., Divekar, D.P., Beaton, L., Hogan, J.J., et al. (2011). Foxp3+ follicular regulatory T cells control the germinal center response. Nat. Med. *17*, 975–982.

Ma, C.S., Deenick, E.K., Batten, M., and Tangye, S.G. (2012). The origins, function, and regulation of T follicular helper cells. J. Exp. Med. *209*, 1241–1253.

MacLennan, I.C., Toellner, K.M., Cunningham, A.F., Serre, K., Sze, D.M., Zúñiga, E., Cook, M.C., and Vinuesa, C.G. (2003). Extrafollicular antibody responses. Immunol. Rev. *194*, 8–18.

Malissen, M., Gillet, A., Ardouin, L., Bouvier, G., Trucy, J., Ferrier, P., Vivier, E., and Malissen, B. (1995). Altered T cell development in mice with a targeted mutation of the CD3-epsilon gene. EMBO J. *14*, 4641–4653.

McHeyzer-Williams, M., Okitsu, S., Wang, N., and McHeyzer-Williams, L. (2011). Molecular programming of B cell memory. Nat. Rev. Immunol. *12*, 24–34.

Murphy, K.M. (2011). Comment on "Activation of β-catenin in dendritic cells regulates immunity versus tolerance in the intestine". Science *333*, 405.

Nakayamada, S., Kanno, Y., Takahashi, H., Jankovic, D., Lu, K.T., Johnson, T.A., Sun, H.W., Vahedi, G., Hakim, O., Handon, R., et al. (2011). Early Th1 cell differentiation is marked by a Tfh cell-like transition. Immunity *35*, 919–931.

Nurieva, R.I., Chung, Y., Hwang, D., Yang, X.O., Kang, H.S., Ma, L., Wang, Y.H., Watowich, S.S., Jetten, A.M., Tian, Q., and Dong, C. (2008). Generation of T follicular helper cells is mediated by interleukin-21 but independent of T helper 1, 2, or 17 cell lineages. Immunity *29*, 138–149.

Nurieva, R.I., Chung, Y., Martinez, G.J., Yang, X.O., Tanaka, S., Matskevitch, T.D., Wang, Y.H., and Dong, C. (2009). Bcl6 mediates the development of T follicular helper cells. Science *325*, 1001–1005.

O'Shea, J.J., and Paul, W.E. (2010). Mechanisms underlying lineage commitment and plasticity of helper CD4+ T cells. Science *327*, 1098–1102.

Oestreich, K.J., Mohn, S.E., and Weinmann, A.S. (2012). Molecular mechanisms that control the expression and activity of Bcl-6 in TH1 cells to regulate flexibility with a TFH-like gene profile. Nat. Immunol. *13*, 405–411.

Oxenius, A., Bachmann, M.F., Zinkernagel, R.M., and Hengartner, H. (1998). Virus-specific MHC-class II-restricted TCR-transgenic mice: effects on humoral and cellular immune responses after viral infection. Eur. J. Immunol. *28*, 390–400.

Pepper, M., Pagán, A.J., Igyártó, B.Z., Taylor, J.J., and Jenkins, M.K. (2011). Opposing signals from the Bcl6 transcription factor and the interleukin-2 receptor generate T helper 1 central and effector memory cells. Immunity *35*, 583–595.

Phan, T.G., Amesbury, M., Gardam, S., Crosbie, J., Hasbold, J., Hodgkin, P.D., Basten, A., and Brink, R. (2003). B cell receptor-independent stimuli trigger immunoglobulin (Ig) class switch recombination and production of IgG autoantibodies by anergic self-reactive B cells. J. Exp. Med. *197*, 845–860.

Poholek, A.C., Hansen, K., Hernandez, S.G., Eto, D., Chandele, A., Weinstein, J.S., Dong, X., Odegard, J.M., Kaech, S.M., Dent, A.L., et al. (2010). In vivo regulation of Bcl6 and T follicular helper cell development. J. Immunol. *185*, 313–326.

Probst, H.C., Tschannen, K., Odermatt, B., Schwendener, R., Zinkernagel, R.M., and Van Den Broek, M. (2005). Histological analysis of CD11c-DTR/GFP mice after in vivo depletion of dendritic cells. Clin. Exp. Immunol. *141*, 398–404.

Qi, H., Cannons, J.L., Klauschen, F., Schwartzberg, P.L., and Germain, R.N. (2008). SAP-controlled T-B cell interactions underlie germinal centre formation. Nature *455*, 764–769.

Reboldi, A., Coisne, C., Baumjohann, D., Benvenuto, F., Bottinelli, D., Lira, S., Uccelli, A., Lanzavecchia, A., Engelhardt, B., and Sallusto, F. (2009). C-C chemokine receptor 6-regulated entry of TH-17 cells into the CNS through the choroid plexus is required for the initiation of EAE. Nat. Immunol. *10*, 514–523.

Recher, M., Lang, K.S., Hunziker, L., Freigang, S., Eschli, B., Harris, N.L., Navarini, A., Senn, B.M., Fink, K., Lötscher, M., et al. (2004). Deliberate removal of T cell help improves virus-neutralizing antibody production. Nat. Immunol. *5*, 934–942.

Schaerli, P., Willimann, K., Lang, A.B., Lipp, M., Loetscher, P., and Moser, B. (2000). CXC chemokine receptor 5 expression defines follicular homing T cells with B cell helper function. J. Exp. Med. *192*, 1553–1562.

Schwickert, T.A., Lindquist, R.L., Shakhar, G., Livshits, G., Skokos, D., Kosco-Vilbois, M.H., Dustin, M.L., and Nussenzweig, M.C. (2007). In vivo imaging of germinal centres reveals a dynamic open structure. Nature *446*, 83–87.

Tangye, S.G., and Tarlinton, D.M. (2009). Memory B cells: effectors of long-lived immune responses. Eur. J. Immunol. *39*, 2065–2075.

Tsuji, M., Komatsu, N., Kawamoto, S., Suzuki, K., Kanagawa, O., Honjo, T., Hori, S., and Fagarasan, S. (2009). Preferential generation of follicular B helper T cells from Foxp3+ T cells in gut Peyer's patches. Science *323*, 1488–1492.

Victora, G.D., and Nussenzweig, M.C. (2012). Germinal centers. Annu. Rev. Immunol. *30*, 429–457.

Victora, G.D., Schwickert, T.A., Fooksman, D.R., Kamphorst, A.O., Meyer-Hermann, M., Dustin, M.L., and Nussenzweig, M.C. (2010). Germinal center dynamics revealed by multiphoton microscopy with a photoactivatable fluorescent reporter. Cell *143*, 592–605.

Vinuesa, C.G., and Cyster, J.G. (2011). How T cells earn the follicular rite of passage. Immunity *35*, 671–680.

Vinuesa, C.G., Linterman, M.A., Goodnow, C.C., and Randall, K.L. (2010). T cells and follicular dendritic cells in germinal center B-cell formation and selection. Immunol. Rev. *237*, 72–89.

Vogelzang, A., McGuire, H.M., Yu, D., Sprent, J., Mackay, C.R., and King, C. (2008). A fundamental role for interleukin-21 in the generation of T follicular helper cells. Immunity *29*, 127–137.

Wollenberg, I., Agua-Doce, A., Hernández, A., Almeida, C., Oliveira, V.G., Faro, J., and Graca, L. (2011). Regulation of the germinal center reaction by Foxp3+ follicular regulatory T cells. J. Immunol. *187*, 4553–4560.

Yu, D., Rao, S., Tsai, L.M., Lee, S.K., He, Y., Sutcliffe, E.L., Srivastava, M., Linterman, M., Zheng, L., Simpson, N., et al. (2009). The transcriptional repressor Bcl-6 directs T follicular helper cell lineage commitment. Immunity *31*, 457–468.

Yusuf, I., Kageyama, R., Monticelli, L., Johnston, R.J., Ditoro, D., Hansen, K., Barnett, B., and Crotty, S. (2010). Germinal center T follicular helper cell IL-4 production is dependent on signaling lymphocytic activation molecule receptor (CD150). J. Immunol. *185*, 190–202.